

## On direction of radiation induced by a horseshoe type cyclotron instability

I. Vorgul<sup>1</sup>, B.J. Kellet<sup>2</sup>, R.A. Cairns<sup>1</sup>, R. Bingham<sup>2,3</sup>, K. Ronald<sup>3</sup>, D.C. Speirs<sup>3</sup>,  
S.L. McConville<sup>3</sup>, K.M. Gillespie<sup>3</sup> and A.D.R. Phelps<sup>3</sup>

<sup>1</sup> *School of Mathematics and Statistics, University of St Andrews, UK*

<sup>2</sup> *STFC Rutherford Appleton Laboratory, Chilton, Didcot, UK*

<sup>3</sup> *SUPA, Department of Physics, University of Strathclyde, Glasgow, UK*

Recent observations of auroral kilometric radiation (AKR) [1] as well as laboratory experiments [2], computer simulations [3,4] and analytic studies [5] suggest that AKR is generated in elongated regions of low plasma density in a direction which is initially at a small upwards angle to the direction of the magnetic field, and so in the opposite direction to the beam generating the radiation. We have previously suggested that the radiation is generated by a horseshoe type distribution [6] and we have shown that the main features of AKR can be produced in laboratory experiments [2]. Fig. 1 shows a computer simulation result (generated using the KARAT simulation code) clearly showing the backward propagation. Here we show that the backward propagation of the fastest growing wave can be given a simple explanation in terms of the basic properties of the horseshoe instability.

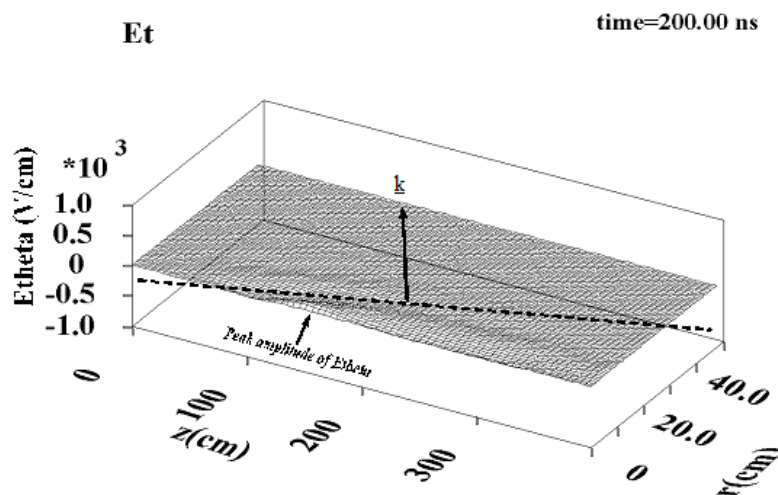


Figure 1: Circular beam simulations in KARAT. The electric field contours show the outward propagating wave at a small angle to the normal to the beam direction (left to right)

The instability is generated by a population inversion of electrons in the direction perpendicular to the magnetic field with the resonant electrons which give rise to the instability (close to

the cyclotron frequency) satisfying

$$\omega - k_{\parallel}v_{\parallel} = \frac{\omega_c}{\gamma}. \quad (1)$$

If we take a typical horseshoe distribution, produced from an initial Maxwellian with drift speed  $0.25c$ , thermal velocity  $0.015c$  and magnetic compression by a factor 15, then a contour plot of  $\frac{\partial f}{\partial v_{\perp}}$  (restricted to regions where it is positive) is shown in Fig. 2. Velocities in what follows will be in units of  $c$  and frequencies in units of  $\omega_c$ .

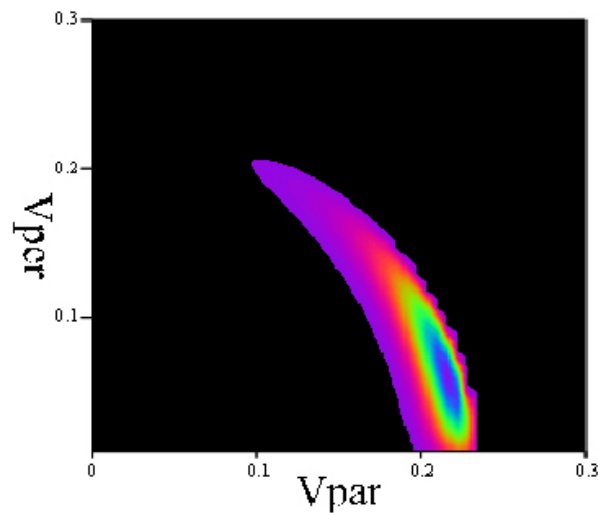


Figure 2: Contour plot of positive gradient regions of horseshoe distribution

This shows that maximum growth can be expected when the resonance curve passes through a fairly restricted area in velocity space. The shape of the resonance curves is indicated in Fig. 3, plotted for  $\omega = 0.97\omega_c$  and three different values of  $n_{\parallel} = \frac{k_{\parallel}c}{\omega}$ .

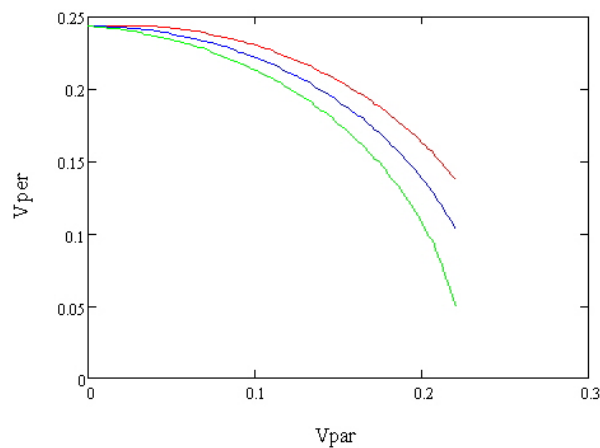


Figure 3: Resonance curves for  $n_{\parallel} = 0.02$  (red), 0 (blue),  $-0.02$  (green)

The point to note is that for positive  $n_{||}$  the curve lies above the  $n_{||} = 0$  curve, while for negative  $n_{||}$  it lies below. The other relevant thing to notice is that increasing the frequency moves the whole curve downwards, starting at a lower point at  $v_{||} = 0$ . Combining these two pieces of information it can be seen that in order for the resonance curve to pass through the region of maximum  $\frac{\partial f}{\partial v_{\perp}}$  it must have a higher frequency when  $n_{||}$  is positive than when  $n_{||}$  is zero, so that the lower starting point at  $v_{||} = 0$  compensates for the smaller downwards curvature. For negative  $n_{||}$  maximum growth is to be expected at a lower frequency. This is illustrated by Fig. 4, in which the perpendicular gradient along the resonance curve is shown as a function of  $v_{||}$  and of frequency. This shows the maximum value of the gradient occurring at higher frequencies when  $n_{||}$  is positive.

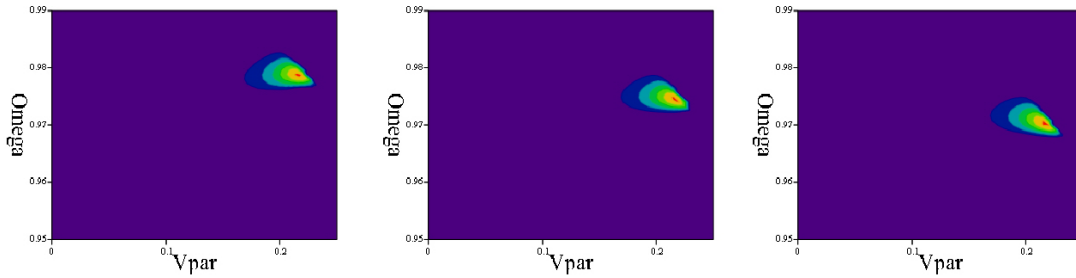


Figure 4: Contour plots of perpendicular gradient along resonance curve as a function of  $v_{||}$  and frequency. From left to right the values of  $n_{||}$  are 0.02, 0 and  $-0.02$

The positive gradient, integrated along the resonant paths, does not vary significantly when resonant paths passing through the regions of maximum gradient are chosen. However, it needs to be noted that the growth rate is approximately

$$\omega_{im} = \frac{\text{Im}(D)}{\frac{\partial}{\partial \omega}(\text{Re}(D))} \quad (2)$$

where  $D = 0$  is the dispersion relation. As a simple approximation to  $\text{Re}(D)$  we just take the cold plasma result at perpendicular incidence, a reasonable approximation if  $n_{||}$  is small and also the Larmor radius is small compared to the perpendicular wavelength. The value of  $\frac{\partial D}{\partial \omega}$  as a function of frequency is shown in Fig. 5, for  $\omega_p = 0.1\omega_c$ , plasma frequencies well below the electron cyclotron frequency being characteristic of regions of AKR emission.

The crucial point to notice is that because of the proximity to the upper hybrid resonance, where  $D$  has a singularity, the gradient increases rapidly with frequency. Even though the value of  $\text{Im}(D)$  is very much the same for each combination of  $\omega$  and  $n_{||}$  which maximizes the growth rate, the decreasing gradient of  $\text{Re}(D)$  favours the lower frequencies which correspond to negative values of  $n_{||}$ . On the other hand if the negative value of  $n_{||}$  is too large the resonance

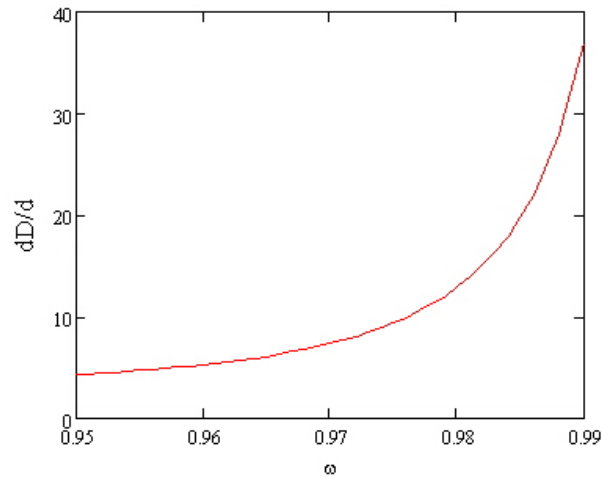


Figure 5: Gradient with respect to frequency of dispersion function

curves are no longer closely aligned along the elongated region of maximum gradient indicated in Fig. 2 and the growth rate then falls off. More detailed calculations estimating the value of  $\text{Im}(D)$  by integrating along the resonance curve, suggest that the maximum growth rate should occur at an angle of a few degrees to the magnetic field in the direction opposite to the electron beam, in accord with observation and simulation.

### Acknowledgement.

This work was supported by the UK Engineering and Physical Sciences Research Council

### References

- [1] J.D. Menietti *et al.*, Journal of Geophys. Res., **116**, A12219, doi:10.1029/2011JA017168 (2011).
- [2] D.C. Speirs *et al.*, Phys Plasmas, **17** (6), 069901 (2010).
- [3] K. Ronald *et al.*, Plasma Phys Contr Fusion, **53**, 074015 (2011).
- [4] K.M. Gillespie *et al.*, at this Proceedings (2012).
- [5] I. Vorgul *et al.*, Phys Plasmas, **18**, 056501 (2011).
- [6] R. Bingham and R.A. Cairns, Physics of Plasmas, **7**, 3089, (2000).